

# Preparation and characterization of the square-based pyramidal cluster anion $[\text{H}_2\text{Ru}_5(\text{CO})_{14}(\mu_4\text{-COH})]$

Jane R. Galsworthy<sup>a</sup>, Catherine E. Housecroft<sup>a,b,\*</sup>, Robert L. Ostrander<sup>c</sup>, Arnold L. Rheingold<sup>c,\*</sup>

<sup>a</sup> University Chemical Laboratory, Lensfield Road, Cambridge CB1 2EW, UK

<sup>b</sup> Institut für Anorganische Chemie, Spitalstrasse 51, CH-4056 Basel, Switzerland

<sup>c</sup> Department of Chemistry, University of Delaware, Newark DE 19716, USA

Received 27 September 1994

## Abstract

The new compound  $[\text{PPN}][\text{H}_2\text{Ru}_5(\text{CO})_{14}(\mu_4\text{-COH})]$ ,  $[\text{PPN}][\mathbf{1}]$ , (PPN = bis(triphenylphosphine) iminium) is a product in several cluster expansion reactions which use triruthenaboranes as precursors, although the yields are not high. An X-ray diffraction study has shown that in the anion  $\mathbf{1}$  has a square-based pyramidal framework of ruthenium atoms. With the square face capped by a  $\mu_4\text{-COH}$  group. Studies of the reactivity of  $\mathbf{1}$  have been carried out, but have not shown  $\mathbf{1}$  to be a ready precursor to an  $\text{Ru}_5\text{C}$ -carbido species as had been expected.

**Keywords:** Ruthenium; Carbonyl; Cluster; Crystal structure

## 1. Introduction

In carrying out reactions aimed at increasing the nuclearity of transition metallaborane clusters [1] we have isolated a pentaruthenium, non-boron-containing product. We initially formulated this compound as  $[\text{PPN}][\text{HRu}_5(\text{CO})_{15}]$  [2], but detailed examination of the crystal structure of the anion and an evaluation of the number of valence electrons available led us to take a closer look at the compound. The compound is formed in a range of reactions in varying yields and has now been identified as  $[\text{PPN}][\text{H}_2\text{Ru}_5(\text{CO})_{14}(\mu_4\text{-COH})]$ ,  $[\text{PPN}][\mathbf{1}]$ . The anion  $\mathbf{1}$  warrants attention because it exhibits a square-based pyramidal metal cluster geometry, the square face of which supports a quadruply bridging COH-group. In this paper we describe methods of preparing  $[\text{PPN}][\mathbf{1}]$ , and the spectroscopic and structural characterisation of anion  $\mathbf{1}$ . We have also explored the reactions of  $\mathbf{1}$ , because it would appear to be an obvious precursor to the known carbide cluster  $\text{Ru}_5(\text{CO})_{15}\text{C}$  [3,4].

## 2. Experimental details

### 2.1. General

Fourier-transform NMR spectra were recorded on a Bruker WM 250 spectrometer. <sup>1</sup>H shifts are reported with respect to  $\delta$  0 for  $\text{Me}_4\text{Si}$ . Solution IR spectra were recorded on a Perkin-Elmer FT 1710 spectrophotometer, and fast atom bombardment (FAB) mass spectra were obtained with Kratos instruments with NOBA as matrix.

All reactions were carried out under argon by use of standard Schlenk methods. Solvents were pre-dried and distilled under  $\text{N}_2$ . Separations were carried out by thin layer plate chromatography on Kieselgel 60-PF-254 (Merck). The compounds  $[\text{Cp}^*\text{RuCl}_2]_n$  and  $(\eta^6\text{-MeC}_6\text{H}_4\text{-4-CHMe}_2)\text{RuCl}_2$  were used as received (Aldrich) and  $[\text{PPN}][\text{Ru}_3(\text{CO})_9\text{BH}_4]$  [5] and  $\text{W}(\text{CO})_4(\text{MeCN})_2$  [6] were prepared by published procedures.

### 2.2. Preparation of $[\text{PPN}][\mathbf{1}]$

#### 2.2.1. Method 1

We previously described the preparation of the spiked butterfly cluster  $\text{H}_2\text{Ru}_5(\text{CO})_{13}\text{Cp}^*\text{BH}_2$  by the

\* Corresponding authors.

reaction between  $[\text{PPN}][\text{Ru}_3(\text{CO})_9\text{BH}_4]$  and  $[\text{Cp}^*\text{-RuCl}_2]_n$ . A by-product of this reaction is  $[\text{PPN}][\mathbf{1}]$  (4.5% yield), although we originally proposed that this compound was  $[\text{PPN}][\text{HRu}_5(\text{CO})_{15}]$  (see Discussion) [1].

### 2.2.2. Method 2

The  $[\text{PPN}][\text{Ru}_3(\text{CO})_9\text{BH}_4]$  (0.11 g, 0.10 mmol) and  $[(\eta^6\text{-MeC}_6\text{H}_4\text{-4-CHMe}_2)\text{RuCl}_2]_2$  (0.06 g, 0.10 mmol) were each separately dissolved in  $\text{CH}_2\text{Cl}_2$  (6  $\text{cm}^3$ ) and the first solution was added to the second. During 1 hr of stirring, the solution turned brown. The products were separated by TLC; the initial elution with hexane enabled isolation of  $\text{HRu}_4(\text{CO})_{12}\text{BH}_2$  [7,8] and  $\text{HRu}_4(\text{CO})_9(\eta^6\text{-MeC}_6\text{H}_4\text{-4-CHMe}_2)\text{BH}_2$  [9]. Further elution with  $\text{CH}_2\text{Cl}_2$ :hexane (2:1) then gave three fractions. The first (yellow) band contained a mixture of boron-containing products, (by  $^{11}\text{B}$  NMR spectroscopy); it was not separated further because the amount of material was so small. The second (major) fraction was  $[\text{PPN}][\text{Ru}_6(\text{CO})_{17}\text{B}]$  [10–12], and the third was identified as  $[\text{PPN}][\text{H}_2\text{Ru}_5(\text{CO})_{14}(\mu_4\text{-COH})]$ ,  $[\text{PPN}][\mathbf{1}]$  (ca. 5%).

$[\text{PPN}][\mathbf{1}]$ :  $^1\text{H}$  NMR (298 K,  $\text{CDCl}_3$ )  $\delta$  7.7–7.3 (m,  $\text{PPN}^+$ ), –13.5 (s, Ru–H–Ru); IR ( $\text{CH}_2\text{Cl}_2$ ,  $\text{cm}^{-1}$ ) 2068w, 2025sh, 2016 vs, 2006vs, 1967m(br), 1810w(br), 1781w(br); FAB-MS  $m/z$  928 ( $\text{P}^-$ ) with four CO losses (Calc. for  $^{12}\text{C}_{15}^{1}\text{H}_3^{16}\text{O}_{15}^{101}\text{Ru}_5$  928).

### 2.2.3. Method 3

To a solution of  $[\text{PPN}][\text{Ru}_3(\text{CO})_9\text{BH}_4]$  (0.22 g, 0.20 mmol) in  $\text{CH}_2\text{Cl}_2$  (5  $\text{cm}^3$ ) was added a solution of  $\text{W}(\text{CO})_4(\text{MeCN})_2$  (0.04 g, 0.10 mmol) in MeCN (5  $\text{cm}^3$ ). The reaction solution darkened from orange-red to orange-brown during 6 h of stirring at room temperature. The products were separated by TLC, with  $\text{CH}_2\text{Cl}_2$ :hexane (2:1) as eluant. The first two fractions (yellow) were identified as  $\text{Ru}_3(\text{CO})_9\text{BH}_5$  [13] and  $\text{H}_4\text{Ru}_4(\text{CO})_{12}$  [14], respectively. Three fractions followed that we have been unable to fully characterise. The sixth (orange, ca. 10%) and seventh (brown, ca. 40%) fractions were  $[\text{PPN}][\text{H}_2\text{Ru}_6(\text{CO})_{18}\text{B}]$  [11,12] and  $[\text{PPN}][\text{Ru}_6(\text{CO})_{17}\text{B}]$  [10–12]. The final band (pale peach coloured, ca. 10%) was identified as  $[\text{PPN}][\mathbf{1}]$ .

The reaction follows a parallel path when  $\text{W}(\text{CO})_4(\text{MeCN})_2$  is replaced by  $\text{Mo}(\text{CO})_4(\text{MeCN})_2$ .

### 2.3. Reaction of $[\text{PPN}][\mathbf{1}]$ with $\text{CF}_3\text{COOH}$

To a solution of  $[\text{PPN}][\mathbf{1}]$  (0.07 g, 0.05 mmol) in  $\text{CH}_2\text{Cl}_2$  (3  $\text{cm}^3$ ) was added an excess (0.1  $\text{cm}^3$ ) of  $\text{CF}_3\text{COOH}$ . The solution was stirred for 45 min during which the colour changed from pink-brown to brown. No characterisable product could be isolated.

### 2.4. Reaction of $[\text{PPN}][\mathbf{1}]$ with $\text{CF}_3\text{COOH}$ and CO

Carbon monoxide (1 atm) was bubbled for 30 min through a solution of  $[\text{PPN}][\mathbf{1}]$  (0.07 g, 0.05 mmol) in  $\text{CH}_2\text{Cl}_2$  (10  $\text{cm}^3$ ). An excess (0.1  $\text{cm}^3$ ) of  $\text{CF}_3\text{COOH}$  was added while the flow of carbon monoxide was continued. The solution was stirred for 1 h with a continuous flow of CO, during which the colour changed from pink-brown to brown. The products of the reaction were separated by TLC with  $\text{CH}_2\text{Cl}_2$ :hexane (1.5:1) as eluant. The first fraction eluted was  $\text{H}_4\text{Ru}_4(\text{CO})_{12}$  [14]; the major product,  $[\text{PPN}][\mathbf{2}]$ , was collected as the second (brown) fraction.

$[\text{PPN}][\mathbf{2}]$ :  $^1\text{H}$  NMR (298 K,  $\text{CDCl}_3$ )  $\delta$  7.7–7.3 (m,  $\text{PPN}^+$ ), –17.5 (s, Ru–H–Ru); IR ( $\text{CH}_2\text{Cl}_2$ ,  $\text{cm}^{-1}$ ) 2069w, 2030vs, 2018 m(sh), 1997s, 1818w; FAB-MS  $m/z$  954 ( $\text{P}^-$ ) with six CO losses (see text).

### 2.5. X-ray structural determination

Crystallographic data for  $[\text{PPN}][\mathbf{1}]$  are given in Table 1. A specimen mounted on a glass fibre was shown photographically to possess  $\bar{1}$  Laue symmetry. A semi-empirical correction for absorption used 216  $\psi$ -scan reflections. The structure was solved by direct methods. All non-hydrogen atoms were refined anisotropically, and the hydrogen atoms were treated as idealized. The centrosymmetric space group  $P\bar{1}$  was confirmed by the successful refinement.

All computations used SHELXTL-PLUS V4.2 software [15]. Atomic coordinates for  $[\text{PPN}][\mathbf{1}]$  are given in Table 2. A complete list of bond lengths and angles, and

Table 1  
Crystallographic data for  $[\text{PPN}][\mathbf{1}]$

Crystal data	
Formula	$\text{C}_{51}\text{H}_{33}\text{NO}_{15}\text{P}_2\text{Ru}_5$
Formula weight	1467.1
Crystal color and habit	deep-red block
Crystal size, mm	0.45 × 0.50 × 0.55
Crystal system	triclinic
Space group	$P\bar{1}$
$a, b, c, \text{Å}$	9.030(2), 16.382(4), 19.575(5)
$\alpha, \beta, \gamma, \text{deg}$	71.40(2), 76.67(2), 87.42(2)
$V, \text{Å}^3$	2669.3(9)
$Z$	2
$D(\text{calc}), \text{g cm}^{-3}$	1.825
$\mu(\text{Mo K}\alpha), \text{cm}^{-1}$	15.09
Data collection	
Diffractionmeter	Siemens P4 (Mo K $\alpha$ )
Reflections collected	16004 (max $2\theta = 60^\circ$ )
Independent reflections	15580
Observed reflections	8952 ( $5\sigma F$ )
Min./Max. transmission	0.539/0.708
Refinement	
$R(F), R(wF), \%$	4.06, 5.35
Data/parameter	13.3
$\Delta\rho(\text{max}), \text{e Å}^{-3}$	0.77

Table 2  
Atomic coordinates ( $\times 10^4$ ) and isotropic thermal parameters ( $\text{\AA}^2 \times 10^3$ ) for [PPN][1]

Atom	x	y	z	$U_{\text{eq}}^a$
Ru(1)	5420.5(5)	6464.8(3)	3153.5(3)	36.1(2)
Ru(2)	4807.4(5)	4696.4(3)	3194.6(2)	35.1(1)
Ru(3)	6265.1(5)	5819.1(3)	1851.4(2)	39.2(2)
Ru(4)	3961.3(5)	6942.3(3)	1949.0(2)	35.3(1)
Ru(5)	2382.1(5)	5819.8(3)	3248.0(2)	35.6(2)
O(1)	2290(8)	3373(4)	3645(4)	120(4)
O(2)	6087(6)	3821(3)	4568(3)	72(2)
O(3)	6780(9)	3695(4)	2294(3)	108(3)
O(4)	6470(9)	5199(5)	542(4)	128(4)
O(5)	9715(6)	5988(5)	1473(4)	120(4)
O(6)	6835(6)	7593(3)	721(3)	86(2)
O(7)	7759(8)	7882(4)	2212(4)	114(3)
O(8)	7106(7)	5800(4)	4409(3)	81(3)
O(9)	3464(7)	7748(3)	3762(3)	83(3)
O(10)	4361(9)	8842(3)	1745(4)	115(4)
O(11)	2451(6)	7315(4)	656(3)	76(2)
O(12)	831(7)	7477(4)	2689(3)	96(3)
O(13)	793(7)	5974(4)	4754(3)	82(3)
O(14)	-465(6)	4901(4)	3268(4)	99(3)
O(15)	3078(7)	5067(4)	1874(3)	94(3)
C(1)	3204(10)	3905(5)	3498(5)	82(4)
C(2)	5642(7)	4141(4)	4056(3)	47(2)
C(3)	6137(10)	4204(5)	2537(4)	72(4)
C(4)	6369(9)	5440(5)	1040(4)	70(3)
C(5)	8430(8)	5911(5)	1637(4)	69(3)
C(6)	6107(8)	7068(4)	1232(4)	55(3)
C(7)	6895(8)	7345(5)	2550(4)	65(3)
C(8)	6471(8)	6040(4)	3949(4)	53(3)
C(9)	4148(8)	7258(4)	3535(4)	56(3)
C(10)	4184(9)	8128(4)	1819(4)	62(3)
C(11)	2996(7)	7149(4)	1145(4)	49(2)
C(12)	1796(8)	6974(4)	2696(4)	56(3)
C(13)	1393(7)	5907(4)	4197(4)	53(3)
C(14)	626(7)	5251(5)	3251(4)	63(3)
C(15)	3818(6)	5504(3)	2289(3)	34(2)
P(1)	8525(1)	1273(1)	1669(1)	30(1)
P(2)	7150(2)	523(1)	3305(1)	31(1)
N	8293(5)	795(3)	2525(3)	39(2)
C(31)	5978(8)	2200(5)	1398(4)	61(3)
C(32)	4611(9)	2328(6)	1195(5)	80(4)
C(33)	4056(9)	1751(6)	932(5)	82(4)
C(34)	4840(8)	1025(6)	885(4)	65(3)
C(35)	6211(7)	877(4)	1097(3)	47(2)
C(36)	6781(6)	1465(4)	1353(3)	38(2)
C(41)	10259(7)	2483(4)	1872(4)	47(2)
C(42)	10955(8)	3287(4)	1683(4)	61(3)
C(43)	10906(9)	3901(5)	1031(5)	73(4)
C(44)	10161(9)	3733(4)	549(4)	65(3)
C(45)	9437(8)	2939(4)	726(3)	50(2)
C(46)	9482(6)	2311(3)	1395(3)	32(2)
C(51)	9708(7)	-275(4)	1549(3)	44(2)
C(52)	10679(8)	-782(4)	1212(3)	50(2)
C(53)	11640(7)	-414(4)	532(4)	48(2)
C(54)	11651(6)	454(4)	180(3)	42(2)
C(55)	10685(6)	975(3)	507(3)	37(2)
C(56)	9725(5)	617(3)	1197(3)	31(2)
C(61)	4540(7)	147(4)	2956(3)	52(3)
C(62)	3013(8)	216(5)	2938(4)	66(3)
C(63)	2122(8)	751(5)	3250(5)	77(4)
C(64)	2702(8)	1234(5)	3577(5)	76(4)
C(65)	4257(7)	1199(4)	3599(4)	58(3)
C(66)	5163(6)	641(4)	3294(3)	38(2)

Table 2b (continued)

Atom	x	y	z	$U_{\text{eq}}$
C(71)	7834(7)	2021(4)	3536(3)	47(2)
C(72)	8333(8)	2498(4)	3909(4)	59(3)
C(73)	8618(9)	2104(5)	4594(4)	67(3)
C(74)	8378(9)	1240(5)	4914(4)	67(3)
C(75)	7901(7)	739(4)	4543(3)	50(2)
C(76)	7630(6)	1128(3)	3857(3)	36(2)
C(82)	6405(11)	-1943(5)	4694(5)	77(4)
C(83)	7795(12)	-2289(5)	4535(5)	81(4)
C(84)	8992(10)	-1821(5)	4015(4)	69(4)
C(85)	8772(8)	-965(4)	3632(4)	53(3)
C(86)	7364(6)	-597(3)	3783(3)	37(2)
C(81)	6186(8)	-1088(4)	4311(4)	58(3)

<sup>a</sup> Equivalent isotropic  $U$  defined as one third of the trace of the orthogonalized  $U_{ij}$  tensor.

tables of anisotropic thermal parameters and hydrogen atom coordinates have been deposited at the Cambridge Crystallographic Data Centre. Selected bond distances and angles in anion **1** are given in Table 3.

### 3. Results and discussion

#### 3.1. Preparation and initial spectroscopic characterisation of [PPN][1]

The reactions of [PPN][Ru<sub>3</sub>(CO)<sub>9</sub>BH<sub>4</sub>] with [Cp<sup>+</sup>RuCl<sub>2</sub>]<sub>n</sub> [1] ( $\eta^6\text{-MeC}_6\text{H}_4\text{-4-CHMe}_2\text{)RuCl}_2$ ]<sub>n</sub>, W(CO)<sub>4</sub>(MeCN)<sub>2</sub> and Mo(CO)<sub>4</sub>(MeCN)<sub>2</sub> lead to, amongst other products, a non-boron-containing cluster anion, **1**, which was isolated as the [PPN]<sup>+</sup> salt. The negative FAB mass spectrum of the compound showed a parent envelope at 928 a.m.u. with an isotopic distribution consistent with the presence of five ruthenium atoms and a formulation for the anion **1** based on [Ru<sub>5</sub>(CO)<sub>15</sub>]. The IR spectrum showed the presence of both terminal and bridging carbonyl ligands. The presence of one or more hydride ligands was suggested by the appearance in the <sup>1</sup>H NMR spectrum of [PPN][1] of a sharp singlet at  $\delta$  - 13.5, in addition to resonances assigned to the [PPN]<sup>+</sup> cation. The sharp signal persisted at low temperatures (195 K). The spectroscopic data were keeping with a possible formula of [PPN][HRu<sub>5</sub>(CO)<sub>15</sub>] [1] for [PPN][1]. By comparison with the analogous compound [PPN][HOs<sub>5</sub>(CO)<sub>15</sub>] [16,17], we expected that the structure of anion **1** would be similar to that of [HOs<sub>5</sub>(CO)<sub>15</sub>]<sup>-</sup>, i.e. a trigonal bipyramidal array of metal atoms; this is consistent with a 72 valence electron count.

#### 3.2. Crystal structure of [PPN][1]

A crystal of [PPN][1], suitable for X-ray analysis, was grown from CH<sub>2</sub>Cl<sub>2</sub> layered with hexane. The molecular structure of anion **1** is shown in Fig. 1, and selected

Table 3  
Selected bond distances and angles in anion 1

Bond distances (Å)			
Ru(1)–Ru(2)	2.946(1)	Ru(1)–Ru(3)	2.991(1)
Ru(1)–Ru(4)	2.841(1)	Ru(1)–Ru(5)	2.929(1)
Ru(2)–Ru(3)	2.751(1)	Ru(2)–Ru(5)	2.801(1)
Ru(3)–Ru(4)	2.729(1)	Ru(4)–Ru(5)	2.732(1)
Ru(2)–C(15)	2.195(5)	Ru(3)–C(15)	2.198(5)
Ru(4)–C(15)	2.237(5)	Ru(5)–C(15)	2.216(6)
C(15)–O(15)	1.511(10)		
Bond angles (deg)			
Ru(2)–Ru(1)–Ru(3)	55.2(1)	Ru(2)–Ru(1)–Ru(4)	83.8(1)
Ru(3)–Ru(1)–Ru(4)	55.7(1)	Ru(2)–Ru(1)–Ru(5)	57.0(1)
Ru(3)–Ru(1)–Ru(5)	82.9(1)	Ru(4)–Ru(1)–Ru(4)	56.5(1)
Ru(3)–Ru(2)–Ru(5)	89.8(1)	Ru(2)–Ru(3)–Ru(4)	89.8(1)
Ru(3)–Ru(4)–Ru(5)	91.7(1)	Ru(2)–Ru(5)–Ru(4)	88.6(1)
Ru(2)–C(15)–Ru(4)	121.5(3)	Ru(3)–C(15)–Ru(5)	125.2(3)
Ru(2)–C(15)–O(15)	118.5(3)	Ru(3)–C(15)–O(15)	116.0(4)
Ru(4)–C(15)–O(15)	119.9(4)	Ru(5)–C(15)–O(15)	118.8(4)

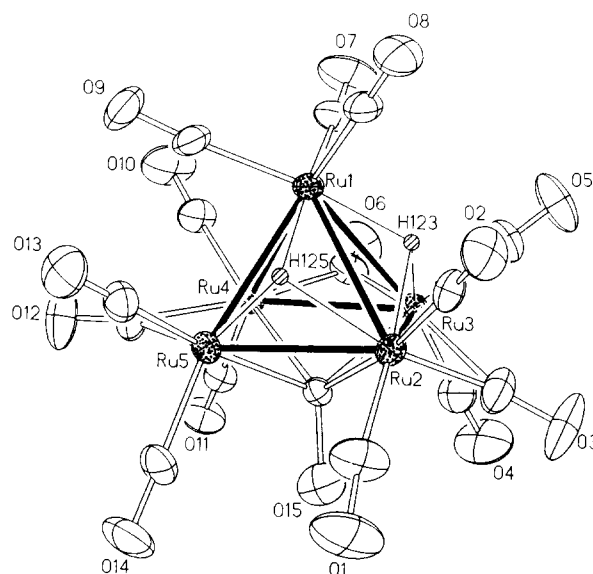


Fig. 1. Molecular structure of anion 1.

bond distances and angles are listed in Table 2. The results confirmed the gross formula of 1, but the unexpected features which emerged were the square-based pyramidal  $Ru_5$ -framework and a  $\mu_4$ -ligand (C(15)O(15) in Fig. 1) associated with the square face. A square-based pyramidal transition metal cage geometry is generally associated with 74 and not 72 valence electrons and thus the structure did not appear to be in keeping with our initial proposal of an  $[HRu_5(CO)_{15}]^-$  anion. In addition, a  $\mu_4$ -bonding environment for a carbonyl ligand, would be, to our knowledge, unprecedented. An inspection of the bond parameters revealed that the distance C(15)–O(15) was 1.511(10) Å. This is *not* consistent with the presence of a simple carbonyl ligand, but, rather, is in keeping with single bond character. We return to this point later.

The apical–basal Ru–Ru distances in anion 1 (average 2.927 Å) are longer than the basal–basal Ru–Ru bond lengths (average 2.753 Å). The apical ruthenium atom, Ru(1), carries three terminal carbonyl ligands and each of the basal ruthenium atoms bears two terminal ligands. Each of the three edges Ru(2)–Ru(3), Ru(3)–Ru(4) and Ru(4)–Ru(5) is bridged by a carbonyl ligand, although in the case of C(3)O(3), the interaction with atom Ru(2) is greater than with Ru(3), rendering the carbonyl ligand semi-bridging in nature. A projection of anion 1, taken through the square face and with the  $\mu_4$ -C(15)O(15) group uppermost, is shown in Fig. 2. The  $\mu_4$ -ligand is symmetrically associated with all four of the basal ruthenium atoms (the Ru–C distances are in the range 2.194(6)–2.237(5) Å). Atom C(15) is raised 1.05 Å above the plane of atoms Ru(2), Ru(3), Ru(4) and Ru(5).

The long C(15)–O(15) distance suggested to us that this was not a carbonyl ligand at all, but may be a  $\mu_4$ -COH group. Examples of cluster-bound COH groups are known (Fig. 3); for example, edge bridging

in  $HFe_3(CO)_{10}(\mu-COH)$  [18] and  $HRu_3(CO)_{10}(\mu-COH)$  [19], capping a metal triangle in  $Co_3(CO)_9(\mu_3-COH)$  [20] and  $Fe_4(CO)_{12}X(\mu_3-COH)$  (X = AuPPh<sub>3</sub> or HgMe) [21], and supported by the tetrairon butterfly framework in  $XFe_4(CO)_{12}(COH)$  (X = H, AuPPh<sub>3</sub> or HgMe) [21–24]. However, to the best of our knowledge, anion 1 represents the first example of a COH-group supported over a square  $M_4$ -face. A  $\mu_4$ -COH ligand provides three electrons to the cluster, and its presence would require that there be two hydride ligands associated with the cluster core. Low tempera-

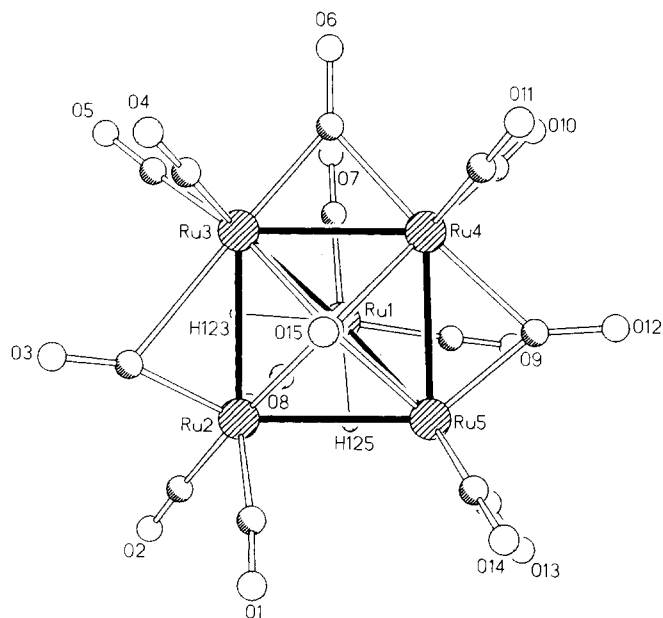


Fig. 2. A projection of anion 1 taken through the Ru(2)Ru(3)Ru(3)-Ru(4) square face and with the  $\mu_4$ -C(15)O(15) group pointing above the plane. Hydrogen atoms are not located.

ture  $^1\text{H}$  NMR spectral data did not prove conclusive in this regard (see above). The difference map supported the presence of two face-capping hydrogen atoms, on the Ru(1,2,3) and Ru(1,2,5) faces.

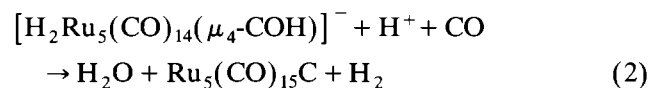
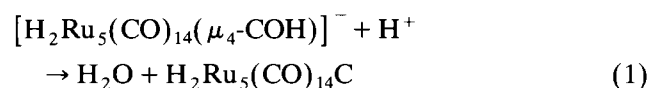
We have been unable to observe an absorption due to an O–H stretching mode in the IR spectrum of [PPN][1], and attempts to carry out H/D substitution have not allowed observation of an absorption assignable to  $\nu(\text{OD})$ .

Other examples of cluster bound COH groups are characterised by downfield resonances in the  $^1\text{H}$  NMR spectrum:  $\text{HFe}_3(\text{CO})_{10}(\mu\text{-COH})$  ( $\delta + 15$  at 193 K and  $+ 13.8$  at 233 K in  $\text{CD}_2\text{Cl}_2$ ), [18]  $\text{HRu}_3(\text{CO})_{10}(\mu\text{-COH})$  ( $\delta + 16.11$  at 213 K in  $\text{CD}_2\text{Cl}_2$ ) [19],  $\text{Co}_3(\text{CO})_9(\mu_3\text{-COH})$  ( $\delta + 11.25$ , 238 K in  $\text{C}_6\text{D}_5\text{CD}_3$ ) [20],  $\text{Fe}_4(\text{CO})_{12}(\text{AuPPh}_3)(\mu_3\text{-COH})$  ( $\delta + 13.7$ , 193 K in  $\text{CD}_2\text{Cl}_2$ ) [21]  $\text{XFe}_4(\text{CO})_{12}(\mu_4, \eta^2\text{-COH})$  ( $\text{X} = \text{H}$ ,  $\delta + 13.2$ ;  $\text{AuPPh}_3$ ,  $\delta + 11.5$ ;  $\text{HgMe}$ ,  $\delta + 12.0$  all in  $\text{CD}_2\text{Cl}_2$  at 193 K) [21–24]. For [PPN][1], no resonance is observed at lower field than the multiplet assigned to the  $\text{PPN}^+$  cation ( $\delta + 7.7\text{--}7.3$ ); no other resonance in the  $^1\text{H}$  NMR spectrum (monitored between room temperature and 195 K) can be assigned to the COH group. We must assume that the resonance for the  $\mu_4\text{-COH}$  group in anion 1 is masked by the signal from the counterion. A lowerfield shift for the OH proton in 1 compared with these in the examples listed above suggests a rather different environment for the hydrogen atom. The C–O bond length in 1 (1.511(10) Å) indicates that the COH group in this compound is alcohol-like. Unlike the previous examples of clusters with bound COH groups, anion 1 is isolable and stable under an inert atmosphere for several weeks.

### 3.3. Reactivity of $[\text{H}_2\text{Ru}_5(\text{CO})_{14}(\mu_4\text{-COH})]^-$

The isolation of the cluster anion  $[\text{H}_2\text{Ru}_5(\text{CO})_{14}(\mu_4\text{-COH})]^-$  was unexpected, but provided us with a system that should be a precursor to the previously characterised carbido cluster  $\text{Ru}_5(\text{CO})_{15}\text{C}$  [3] or to a

related carbido species. The protonation of the multiply bonded carbonyl ligand (the so-called  $\pi\text{-CO}$ ) in  $[\text{HFe}_4(\text{CO})_{13}]^-$  and its transformation to a carbide (and on to methane) via a multiply bonded COH-ligand has been elegantly demonstrated by Shriver and coworkers [21–24]. We argued that, in like manner, the protonation of the  $\mu_4\text{-COH}$  group in 1 should release  $\text{H}_2\text{O}$  according to Eq. (1) and produce the neutral carbido cluster “ $\text{H}_2\text{Ru}_5(\text{CO})_{14}\text{C}$ ”; this is isoelectronic with the known carbide  $\text{Ru}_5(\text{CO})_{15}\text{C}$  [3]. Effectively, the carbon atom of the  $\mu_4\text{-COH}$  group in 1 should be transformed into a  $\mu_4\text{-C}$  atom (a four-electron donor) as the OH unit is protonated and removed as water. The results of protonation with  $\text{CF}_3\text{COOH}$  were not encouraging, and so we performed the same reaction in the presence of CO, expecting the conversion shown in Eq. (2).



However, the brown product of the protonation of 1 in the presence of CO is not neutral. The  $^1\text{H}$  NMR spectrum of the product shows a multiplet due to the  $\text{PPN}^+$  counterion. (This is confirmed in a +FAB mass spectrum of the compound, [PPN][2]). In addition, a sharp resonance in the  $^1\text{H}$  NMR spectrum at  $\delta - 17.5$  indicates the presence of a cluster-bound hydride in anion 2. The –FAB mass spectrum exhibits a parent ion at 954 with six sequential carbonyl losses. The data available suggest that 2 may be formulated as  $[\text{HRu}_5(\text{CO})_{16}]^-$ . This has a 74 valence electron count, consistent with the retention of a square-based pyramidal cluster skeleton on going from 1 to 2. The IR spectrum of 2 suggests the presence of both terminal and bridging CO ligands. It would not be justifiable at present to speculate further on the mechanism of the formation of 2.

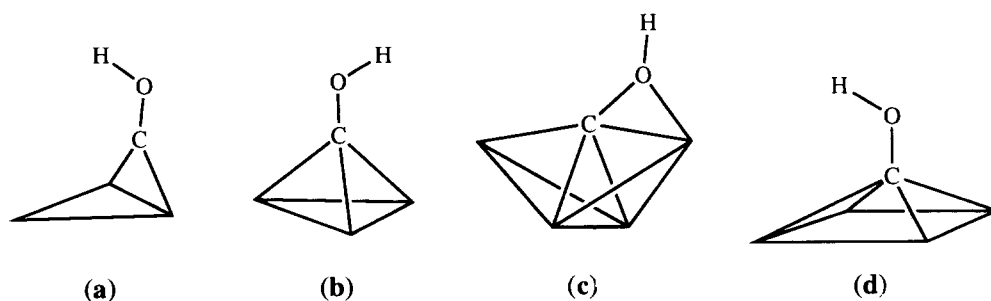


Fig. 3. Modes of bonding of cluster bound COH groups: (a) edge bridging as in  $\text{HM}_3(\text{CO})_{10}(\mu\text{-COH})$  ( $\text{M} = \text{Fe}$  or  $\text{Ru}$ ); (b) capping a metal triangle as in  $\text{Co}_3(\text{CO})_9(\mu_3\text{-COH})$  and  $\text{Fe}_4(\text{CO})_{12}\text{X}(\mu_3\text{-COH})$  ( $\text{X} = \text{AuPPh}_3$  or  $\text{HgMe}$ ); (c) as in the  $\text{M}_4$ -butterfly clusters  $\text{XFe}_4(\text{CO})_{12}(\text{COH})$  ( $\text{X} = \text{H}$ ,  $\text{AuPPh}_3$  or  $\text{HgMe}$ ); (d) in  $[\text{H}_2\text{Ru}_5(\text{CO})_{14}(\mu_4\text{-COH})]^-$ .

## Acknowledgments

We thank the donors of the Petroleum Research Fund, administered by the American Chemical Society for support of this work (grant #25533-AC3), to the EPSRC (formerly SERC) for a studentship to JRG, and to the National Science Foundation for a grant (CHE 9007852) towards the purchase of a diffractometer at the University of Delaware.

## References

- [1] J.R. Galsworthy, C.E. Housecroft and A.L. Rheingold, *Organometallics*, 12 (1993) 4167.
- [2] Footnote 7 in Ref. [1].
- [3] D.H. Farrar, P.F. Jackson, B.F.G. Johnson, J. Lewis, J.N. Nicholls and M. McPartlin, *J. Chem. Soc., Chem. Commun.*, (1981) 415.
- [4] C.R. Eady, B.F.G. Johnson, J. Lewis and T. Matheson, *J. Organomet. Chem.*, 57 (1973) C82.
- [5] S.M. Draper, C.E. Housecroft, A.K. Keep, D.M. Matthews, X. Song and A.L. Rheingold, *J. Organomet. Chem.*, 423 (1992) 241.
- [6] G.R. Dobson, M.F.A. El Sayed, I.W. Stolz and R.K. Sheline, *Inorg. Chem.*, 1 (1962) 526.
- [7] A.K. Chipperfield, C.E. Housecroft and A.L. Rheingold, *Organometallics*, 9 (1990) 681.
- [8] F.-E. Hong, D.A. McCarthy, J.P. White III, C.E. Cottrell and S.G. Shore, *Inorg. Chem.*, 29 (1990) 2874.
- [9]  $\text{HRu}_4(\text{CO})_9(\eta^6\text{-MeC}_6\text{H}_4\text{-4-CHMe}_2\text{)BH}_2$  was identified by its spectral characteristics and their similarity with those of  $\text{HRu}_4(\text{CO})_9(\eta^6\text{-MeC}_6\text{H}_5\text{)BH}_2$ , the structure of which has been confirmed crystallographically: D.M. Matthews, *Ph.D. Thesis*, University of Cambridge, 1992. Full details of a series of related compounds will be reported at a later date.
- [10] F.-E. Hong, T.J. Coffy, D.A. McCarthy and S.G. Shore, *Inorg. Chem.*, 28 (1989) 3284.
- [11] C.E. Housecroft, D.M. Matthews, A.L. Rheingold and X. Song, *J. Chem. Soc., Chem. Commun.*, (1992) 842.
- [12] C.E. Housecroft, D.M. Matthews, A. Waller, A.J. Edwards and A.L. Rheingold, *J. Chem. Soc., Dalton Trans.*, (1993) 3059.
- [13] A.K. Chipperfield and C.E. Housecroft, *J. Organomet. Chem.*, 349 (1988) C17.
- [14] C.R. Eady, B.F.G. Johnson and J. Lewis, *J. Chem. Soc., Dalton Trans.*, (1977) 477.
- [15] G.M. Sheldrick, *Siemens XRD*, Madison, WI, USA.
- [16] C.R. Eady, J.J. Guy, B.F.G. Johnson, J. Lewis and M.C. Malatesta, *J. Chem. Soc., Chem. Commun.*, (1976) 807.
- [17] J.J. Guy and G.M. Sheldrick, *Acta Crystallogr., B* 34 (1978) 1722.
- [18] H.A. Hodali, D.F. Shriver and C.A. Ammlung, *J. Am. Chem. Soc.*, 100 (1978) 5239.
- [19] J.B. Keister, *J. Organomet. Chem.*, 190 (1980) C36.
- [20] G. Fachinetti, *J. Chem. Soc., Chem. Commun.*, (1979) 397.
- [21] C.P. Horwitz and D.F. Shriver, *J. Am. Chem. Soc.*, 107 (1985) 8147.
- [22] K. Whitmire and D.F. Shriver, *J. Am. Chem. Soc.*, 102 (1980) 1456.
- [23] K. Whitmire and D.F. Shriver, *J. Am. Chem. Soc.*, 103 (1981) 6754.
- [24] M.A. Drezdon and D.F. Shriver, *J. Mol. Catal.*, 21 (1983) 81.